On the Radio-frequency Power Requirements of Human MRI

L. Tang[2] and T. S. Ibrahim[1,2]

[1]Departments of Radiology and Bioengineering, University of Pittsburgh
Pittsburgh, Pennsylvania, USA
[2]School of Electrical and Computer Engineering and Bioengineering Center
University of Oklahoma, Norman, Oklahoma, USA

Abstract— In high and ultrahigh field magnetic resonance imaging (MRI) research, computational electromagnetic techniques are now taking an important role in the design and evaluation of MRI radiofrequency (RF) coils. This paper focuses on the RF power requirements and specific absorption rate (SAR) associated with the MRI operation at different field strength. This paper also presents new techniques for achieving high-quality transmit field homogeneity simultaneously with lower total RF power deposition. The studies are done utilizing the finite difference time domain (FDTD) method and the validation of the methods is performed using ultra high field MRI volume coils.

DOI: 10.2529/PIERS061007225757

1. INTRODUCTION

Since magnetic resonance imaging (MRI) technique has been in clinical and research use over the last 30 years, operation at higher magnetic field strength has been a constant goal for the advancement of this diagnostic tool. Although it faces some difficulties such as technical complexity and an increased financial burden, operation at high field MRI is greatly desirable as a result of the associated higher signal-to-noise ratio, contrast-to-noise ratio, and shorter scanning time. Operation at high field MRI and therefore increased frequencies is also associated with complicated interactions of the electromagnetic waves with the tissue since the operating wavelength becomes comparable to or less than the dimensions of the load (human head/body) and RF coil. This can potentially cause severe operational problems such as the presence of inhomogeneous excitation and reception, increased power absorption, and higher local specific absorption rate (SAR).

In human MRI, the total RF power deposition and SAR have been characterized by many researchers [1–4]. For example, at low magnetic field MRI where the wavelength is relatively large compared to the load and RF coil dimensions, quasistatic field approximations were used in the design and assessing the performance of RF coils [5]. Conversely at high or ultrahigh (≥ 7 Tesla) magnetic fields for designing and evaluating RF coils, the significant interactions of the electromagnetic waves with the load invalidate the use of quasistatic approximations and require the application of full wave techniques [6–8]. In this work, a full wave computational electromagnetic method, namely the finite difference time domain (FDTD) technique is implemented in a rigorous fashion by treating the coil and the load as a single system [3] to predict the RF power requirements and SARs of human MRI at high and ultrahigh fields. This computational model is then utilized to design new techniques that can achieve high-quality transmit field homogeneity simultaneously with total RF power deposition lower than that achieved with the standard quadrature excitation [5] for 7 and 9.4 Tesla human MRI.

2. METHODS

2.1. Simulation Model

The model we used is a 16-element TEM resonator [9], which is based on multi-conductor transmission line theory [10], loaded with an anatomically detailed human head mesh [11] as shown in Figure 1. By using the FDTD [12] technique, both the RF coil and the load were modeled as a single system [13] and bounded using perfect matched layers (PML) [14]. In such a modeling approach, the electromagnetic effects on the load due to the coil and on the coil due to the load are included.

From the multi-conductor transmission line theory [10], 9 modes at 9 different frequencies exist in a 16-element TEM coil, where the second mode (mode 1) produces a linearly polarized field (when coil is empty) that can be utilized for imaging. Similar to experiment, the coil was tuned while loaded with the human head mesh by adjusting the gap between the tuning stubs (coil elements).

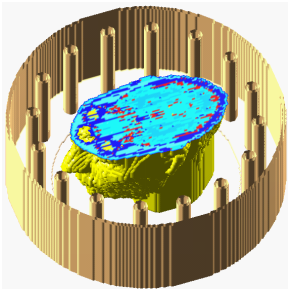

Figure 1: Axial cut of 3D FDTD model system of anatomically detailed human head mesh loaded within a 16-element TEM resonator.

2.2. Power and SAR Calculations

The power input from the RF coil contains the absorbed power by the tissue and the radiated power. It is expressed by Equation (1) derived from the Maxwell equations.

$$P_{\text{input}} = P_{\text{abs}} + P_{\text{rad}} = \frac{\sigma}{2} \iiint_v \left|\vec{E}\right|^2 dv + \frac{1}{2} \iint_s \left(\vec{E} \times \vec{H}^*\right) ds \tag{1}$$

where P_{abs} and P_{rad} are the absorbed and radiated power, σ is conductivity, and $\vec{E}$ and $\vec{H}$ are the electric and magnetic fields respectively. $\iiint_v$ is volume integration over the loaded object, and $\iint_s$ is the closed surface integration that includes the whole system including the coil and the load. Because the RF power absorbed in tissue is related to the flip angle (linearly proportional to one of the circularly polarized components of the transverse magnetic field, known as the B_1^+ field) which directly affects the induced MRI signal, we deliberately only considered the absorbed power in the human head mesh. In numerical simulation, the continuous integration changes to the summation of each FDTD grid as represented by Equation (2).

$$\text{Power} = \sum_i \sum_j \sum_k \left[\frac{1}{2}\sigma_{(i,j,k)} \times \left(E^2_{x_{(i,j,k)}} + E^2_{y_{(i,j,k)}} + E^2_{z_{(i,j,k)}}\right)\right] \tag{2}$$

where $\sigma_{(i,j,k)}$ (S/m) is the conductivity of the FDTD cell at the (i, j, k) location; E_x, E_y and E_z (V/m) are the magnitudes of the electric field components in the x, y, and z directions, respectively; and the summation is performed over the whole volume of the head mesh.

The RF energy during MRI will induce the thermoregulatory imbalance and therefore it is important to monitor the distribution of the energy inside the head. The SAR is intended to indicate the energy absorbed into a tissue of given density by the radio transmitter. In our numerical modeling, it was calculated using the following equation:

$$\text{SAR}_{(i,j,k)} = \frac{1}{2} \frac{\sigma_{(i,j,k)} \left(E^2_{x_{(i,j,k)}} + E^2_{y_{(i,j,k)}} + E^2_{z_{(i,j,k)}}\right)}{\rho_{(i,j,k)}} \tag{3}$$

where $\rho_{(i,j,k)}$ is the tissue density at location (i, j, k). SAR has the unit watt/kilogram.

2.3. Improving the Homogeneity of the B_1^+ Field Distributions

To improve the inhomogeneous excitation (i.e., inhomogeneous B_1^+ field distribution), at 7 and 9.4 Tesla, we utilized an optimization algorithm, based on gradient and genetic algorithms, combined with multi-element/phased-array excitation in order to improve the homogeneity of the B_1^+ field simultaneously with lowering (compared to the standard quadrature excitation) the total RF power deposition in the whole human head.

2.4. Validation of the Electric Field Distributions

To test the validity of the simulation model of the coil-load system, the simulation results were compared to the experimental results obtained utilizing infrared imaging [15]. Figure 2 shows the

infrared measured [15] and FDTD calculated [15] square of transverse electric field distribution of an axial slice inside the 16-strut TEM resonator loaded with a spherical saline phantom and tuned to 340 MHz which corresponds to the Larmor frequency of ^{1}H at 8 Tesla.

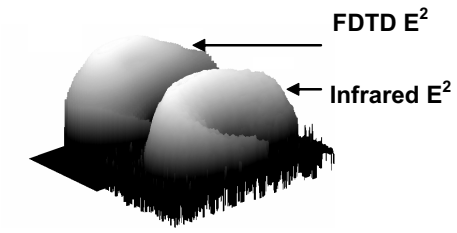

Figure 2: Comparison of infrared images and FDTD calculated electric field distribution at 8 Tesla.

3. RESULTS AND DISSCUSSION

3.1. The Power Absorption Dependency on the External Static Magnetic Field Strength

Using the designed FDTD model, the RF power absorption could be numerically analyzed. Calculations were done at five magnetic field strengths that vary between 4 Tesla and 9.4 Tesla before and after optimization of the homogeneity of the B_1^+ field distribution. The RF power (watts) was scaled to achieve a constant value of 1.174 µ Tesla for the average B_1^+ field intensity in selected slices. The results (Figure 3) interestingly show that higher magnetic fields are not necessary associated with more RF power deposition. For example in Axial Slice 2 and Coronal Slice, compared to 8 Tesla, lower RF power absorption was observed at 9.4 Tesla.

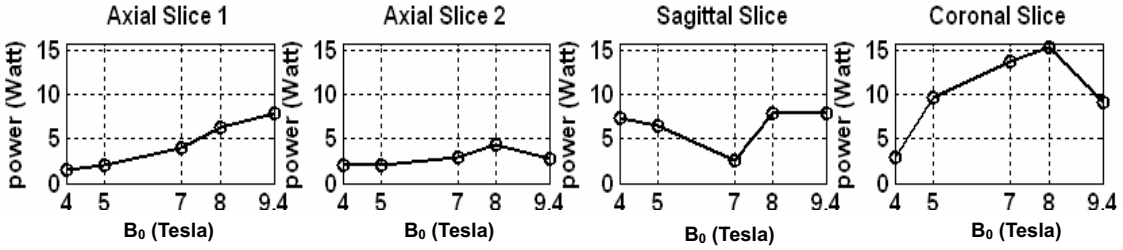

Figure 3: Plots of total power absorbed in the human head as a function of B_0 (external static field) field strength for two axial slices (Axial Slice 1 is a lower brain slice compared to Axial Slice 2) , one sagittal and one coronal slices in order to achieve the same average B_1^+ field intensity and homogeneity (as denoted by the ration of the maximum B_1^+ field intensity divided by the minimum B_1^+ field intensity within the slice of interest).

3.2. Distributions of SAR

The Food and Drug Administration has strict limitations on the peak SAR values and on the continuous MRI examination time. Accurate SAR and total RF power absorption analysis is a must in evaluating new coil designs and excitation techniques. The proposed excitation method demonstrate that a significant improvement in the overall (as denoted by standard deviation) B_1^+

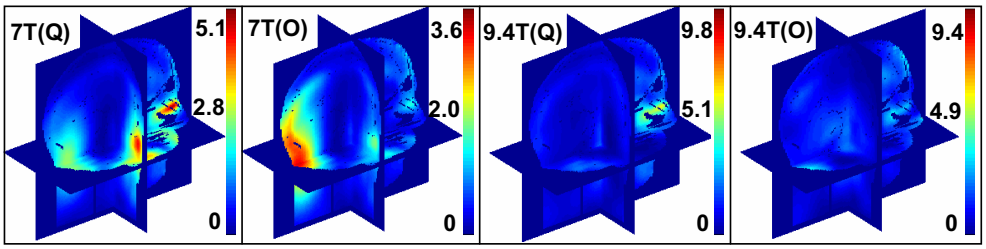

Figure 4: Plots of SAR distributions using quadrature excitation (Q) and optimized (O) B_1^+ field excitation at 7 Tesla (7T) and 9.4 Tesla (9.4T). The corresponding color bars represent the SAR values (watts/kg) for every 10 gm of tissue.

field homogeneity could be achieved while obtaining lower RF power absorptions compared to the standard quadrature excitation. Figure 4 shows some simulation results for SAR distributions at 7 Tesla (7T) and 9.4 Tesla (9.4T) using quadrature excitation (Q) and using optimized excitation (O) over 3-D brain regions. For example at 7 Tesla, compared to the standard quadrature excitation, with optimization of the B_1^+ field over the whole 3-D human brain region:

a. the homogeneity of B_1^+ field distribution was improved by 144%,
b. the peak SAR value was decreased by 29%,
c. and the total RF absorbed power was decreased by 15%.

4. CONCLUSIONS

To obtain high quality images in high and ultra high field human MRI applications, computational electromagnetic techniques, such as FDTD, are taking a significant role in designing the needed RF coils and excitation approaches. Utilizing FDTD method, this work demonstrates that homogenous excitation can be safely achieved at 7 and 9.4 Tesla MRI for human head applications.

REFERENCES

1. Hoult, D. I., "Sensitivity and power deposition in a high-field imaging experiment," *J. Magn. Reson. Imaging*, Vol. 12, No. 1, 46–67, 2000.
2. Collins, C. M. and M. B. Smith, "Signal-to-noise ratio and absorbed power as functions of main magnetic field strength, and definition of "90 degrees" RF pulse for the head in the birdcage coil," *Magn. Reson. Med.*, Vol. 45, No. 4, 684–691, 2001.
3. Ibrahim, T. S., "A numerical analysis of radio-frequency power requirements in magnetic resonance imaging experiment," *IEEE Transactions on Microwave Theory and Techniques*, Vol. 52, No. 8, 1999–2003, 2004.
4. Ibrahim, T. S., R. Lee, B. A. Baertlein, and P.-M. L. Robitaille, "B1 field homogeneity and SAR calculations in the high pass birdcage coil," *Physics in Medicine and Biology*, Vol. 46, 609–619, 2001.
5. Tropp, J., "The theory of the bird-cage resonator," *J. Magn. Reson.*, Vol. 82, 51–62, 1989.
6. Ibrahim, T. S., R. Lee, B. A. Baertlein, A. Kangarlu, and P-M. L. Robitaille, "Application of finite difference time domain method for the design of birdcage RF head coils using multiport excitations," *Magnetic Resonance Imaging*, Vol. 18, 733–742, 2000.
7. Vaughan, J. T., M. Garwood, C. M. Collins, W. Liu, L. DelaBarre, G. Adriany, P. Andersen, H. Merkle, R. Goebel, M. B. Smith, and K. Ugurbil, "7T vs. 4T: RF power, homogeneity, and signal-to-noise comparison in head images," *Magn. Reson. Med.*, Vol. 46, 24–30, Jul. 2001.
8. Wei, Q., F. Liu, L. Xia, and S. Crozier, "An object-oriented designed finite-difference time-domain simulator for electromagnetic analysis and design in MRI–applications to high field analyses," *J. Magn. Reson.*, Vol. 172, 222–30, 2005.
9. Vaughan, J. T., H. P. Hetherington, J. G. Harrison, J. O. Out, J. W. Pan, P. J. Noa, and G. M. Pohost, "High-frequency coils for clinical nuclear magnetic resonance imaging and spectroscopy," *Phy. Med. IX*, 147–153, 1993.
10. Baertlein, B. A., O. Ozbay, T. S. Ibrahim, R. Lee, A. Kangarlu, and P-M. L. Robitaille, "Theoretical model for a MRI radio frequency resonator," *IEEE Trans, Biomed. Eng.*, Vol. 47, 535–546, 2000.
11. Ibrahim, T. S., R. Lee, A. M., Abduljalil, B. A. Baertlein, and P.-M. L. Robitaille, "Effect of RF coil excitation on field inhomogeneity at ultra high fields: A field optimizaed TEM resonator," *Magn. Reson. Imag.*, Vol. 19, 1339–1347, 2001.
12. Yee, K. S., "Numerical solutions of the initial boundary value problems involving Maxwell's equations in isotropic media," *IEEE Trans. Ant. Prop.*, Vol. 14, 302–317, 1966.
13. Chen, J., Z. Feng, and J. M. Jin, "Numerical simulation of SAR and B1-field inhomogeneity of shielded RF coils loaded with the human head," *IEEE Tran. Bio. Eng.*, Vol. 45, No. 5, May 1998.
14. Berenger, J. P., "A perfectly matched layer for the absorption of electromagnetic waves," *J. Computational Physics*, Vol. 114, 185–200, 1994.
15. Ibrahim, T. S. and R. Lee, "Evaluation of MRI RF probes utilizing infrared sensors," *IEEE Tran. Bio. Eng.*, Vol. 53, No. 5, May 2006.